

OPEN ACCESS

EDITED BY

Xiaoquan Rao,
Case Western Reserve University,
United States

REVIEWED BY

Youtao Liu,
MGI Tech Co., Ltd., China
Minhao Fan,
Roche, China
Zhongtian Liu,
University of Pennsylvania, United States

*CORRESPONDENCE

John H. White

✉ john.white@mcgill.ca

SPECIALTY SECTION

This article was submitted to
Molecular Innate Immunity,
a section of the journal
Frontiers in Immunology

RECEIVED 13 December 2022

ACCEPTED 03 January 2023

PUBLISHED 20 January 2023

CITATION

Ismailova A, Salehi-Tabar R, Dimitrov V,
Memari B, Barbier C and White JH (2023)
Identification of a forkhead box protein
transcriptional network induced in
human neutrophils in response to
inflammatory stimuli.
Front. Immunol. 14:1123344.
doi: 10.3389/fimmu.2023.1123344

COPYRIGHT

© 2023 Ismailova, Salehi-Tabar, Dimitrov,
Memari, Barbier and White. This is an open-
access article distributed under the terms of
the [Creative Commons Attribution License
\(CC BY\)](https://creativecommons.org/licenses/by/4.0/). The use, distribution or
reproduction in other forums is permitted,
provided the original author(s) and the
copyright owner(s) are credited and that
the original publication in this journal is
cited, in accordance with accepted
academic practice. No use, distribution or
reproduction is permitted which does not
comply with these terms.

Identification of a forkhead box protein transcriptional network induced in human neutrophils in response to inflammatory stimuli

Aiten Ismailova¹, Reyhaneh Salehi-Tabar¹, Vassil Dimitrov¹,
Babak Memari¹, Camille Barbier¹ and John H. White^{1,2*}

¹Department of Physiology, McGill University, Montreal, QC, Canada, ²Department of Medicine, McGill University, Montreal, QC, Canada

Introduction: Neutrophils represent the largest proportion of circulating leukocytes and, in response to inflammatory stimuli, are rapidly recruited to sites of infection where they neutralize pathogens.

Methods and results: We have identified a novel neutrophil transcription network induced in response to inflammatory stimuli. We performed the first RNAseq analysis of human neutrophils exposed to lipopolysaccharide (LPS), followed by a meta-analysis of our dataset and previously published studies of LPS-challenged neutrophils. This revealed a robustly enhanced transcriptional network driven by forkhead box (FOX) transcription factors. The network is enriched in genes encoding proinflammatory cytokines and transcription factors, including MAFF and ATF3, which are implicated in responses to stress, survival and inflammation. Expression of transcription factors FOXP1 and FOXP4 is induced in neutrophils exposed to inflammatory stimuli, and potential FOXP1/FOXP4 binding sites were identified in several genes in the network, all located in chromatin regions consistent with neutrophil enhancer function. Chromatin immunoprecipitation (ChIP) assays in neutrophils confirmed enhanced binding of FOXP4, but not FOXP1, to multiple sites in response to LPS. Binding to numerous motifs and transactivation of network genes were also observed when FOXP proteins were transiently expressed in HEK293 cells. In addition to LPS, the transcriptional network is induced by other inflammatory stimuli, indicating it represents a general neutrophil response to inflammation.

Discussion: Collectively, these findings reveal a role for the FOXP4 transcription network as a regulator of responses to inflammatory stimuli in neutrophils.

KEYWORDS

lipopolysaccharide, neutrophils, transcriptional regulation, gene expression profiling, innate immunity

Introduction

Neutrophils represent the largest proportion of circulating leukocytes in the blood and are essential to the innate immune response against invading pathogens (1). In response to inflammatory stimuli, neutrophils are rapidly recruited to sites of infection and inflammation where they efficiently bind, engulf and inactivate pathogens. Moreover, these cells secrete chemokines and pro-inflammatory cytokines, which facilitates recruitment and activation of additional neutrophils as well as other immune cells to inflamed tissues (1). Defects in neutrophil antimicrobial processes or a decrease in neutrophil abundance often lead to increased risk of infection or chronic inflammatory or autoimmune conditions such as systemic lupus erythematosus and rheumatoid arthritis (2–6). They are also implicated in the pathogenesis of viral infections; for example, a growing body of evidence supports a link between infiltrating activated neutrophils and increased COVID-19 disease severity (7–9). The killing of invading microorganisms by neutrophils thus necessitates careful control of neutrophil function, as neutropenia renders the body vulnerable to infection, whereas overactivity is associated with inflammatory diseases (1, 10). Moreover, neutrophils can influence cancer progression; they are abundant in tumours and promote tumour development by secreting cytokines and matrix-degrading proteases (10, 11). Consequently, a comprehensive understanding of (dys)regulated molecular signal pathways and transcriptional networks in activated neutrophils is critical for understanding responses to infectious or inflammatory signals.

Bacterial lipopolysaccharide (LPS) is often used as an inflammatory signal, and is capable of inducing several functional responses in neutrophils that contribute to innate immunity, such as altering neutrophil adhesion, respiratory burst, degranulation and motility (12–15). It follows that transcriptional responses play a key role in the stimulation of cytokine and chemokine production in neutrophils. LPS signaling activates transcription factors, such as nuclear factor-kappa B (NF- κ B) and STAT3 (16, 17). Several microarray studies of varying sizes have screened human neutrophil LPS-mediated signal transduction pathways and transcriptional networks (18–26). Despite discrepancies in microarray platforms and doses of LPS treatment, several studies (18–26) have shown that transcripts encoding the pro-inflammatory cytokines and chemokines, IL-1B, IL-6, CCL2, and CCL4 are induced in response to the inflammatory agent.

Here, we performed the first RNA sequencing (RNAseq) analysis of primary human neutrophils to probe the transcriptional responses to LPS on a genome-wide scale, followed by a meta-analysis of LPS-induced neutrophil gene expression profiles. We found that the most robustly enhanced transcriptional network, which is driven by forkhead box transcription factors, consists of genes that encode pro-inflammatory cytokines and transcription factors that are associated with inflammation and stress, such as MAFF and ATF3. Forkhead box transcription factors are characterized by the presence of a highly conserved forkhead DNA-binding domain (27). They possess overlapping binding specificities and are expressed in a cell-specific manner (28). We find that, among forkhead transcription factors, expression of FOXP1 and FOXP4 is enhanced in primary human neutrophils in response to LPS. This leads to enhanced

binding of FOXP4, but not FOXP1, to multiple forkhead box motifs in network genes in neutrophils. Moreover, the network is induced in neutrophils by other inflammatory signals, such as a PKA agonist, GM-CSF and IFN- γ , indicating that it is a component of neutrophil responses to inflammation. These studies reveal a novel transcription network induced in neutrophils in response to inflammatory stimuli.

Results

Gene expression profiling by RNAseq of primary human neutrophils stimulated with LPS

To determine the transcriptomic responses of neutrophils under inflammatory conditions, we performed gene expression profiling by RNAseq in triplicate isolates of primary human neutrophils treated with LPS or vehicle (scheme for experimental protocol; Figure 1A; S1 File). Cells were stimulated with 1 μ g/ml LPS or treated with vehicle for 6 hours to gain insight into primary and secondary effects on gene expression. 1 μ g/ml of LPS was employed in order to mimic systemic inflammation; this dose was shown to induce the greatest ERK phosphorylation in human neutrophils (29). ERK is a subfamily of the mitogen-activated protein kinase (MAPK), which, upon phosphorylation, is involved in signal transduction pathways of inflammation (30, 31) and neutrophil phagocytosis (32). Moreover, 1 μ g/ml of LPS was found to be efficient at halting primary human neutrophil chemotaxis at infectious foci, enabling the cells to exert bactericidal functions at pathogenic sites (33). We then examined the cell signaling canonical pathways, diseases and biological functions as well as upstream transcriptional regulators by pathways analysis (Figure 1A).

LPS treatment resulted in broad changes in mRNA profiles, in which 2565 and 2457 genes were up- and downregulated, respectively, at least 2-fold or greater compared with vehicle ($p \leq 0.05$). The most strongly induced gene was *IL36G*, induced > 11 000 fold, whereas the most strongly repressed gene was *CXCR2* (0.08 fold) (Figure 1B). Up- and downregulated genes with a range of fold regulations were selected for RT/qPCR validation of the RNAseq analysis. We chose genes with a range of LPS-induced fold changes for further validation, for example ranging from *IL36G*, the most strongly induced gene, to *NOD2*, whose expression was induced 2.07-fold by LPS (Figure 1B). We also chose repressed genes *CXCR2*, *CAMP* and *CLEC7A* for further analysis (Figure 1B). Results from RT/qPCR gene expression analysis largely corroborate the expression data generated by RNAseq (Figure 1B). As we used a higher dose of LPS than other studies, we evaluated the effects of differing doses on neutrophil gene expression. Dose-response curves were generated by exposing neutrophils to increasing concentrations of LPS (0, 0.01, 0.1, 1 μ g/ml) for 6 h and assessing the regulation of validated genes by RT/qPCR (Figure 1C). This revealed that the higher dose used in our study did not differ substantially from lower doses in its effects on gene repression (*CAMP*, *CXCR2*), but appears to have been less efficacious in activating gene expression (*IL36G*, *CSF3*, *CXCL8*). Importantly, however, these data suggest that it is unlikely that the higher dose used here led to gene regulatory events that would be absent in other studies that employed lower doses of LPS.

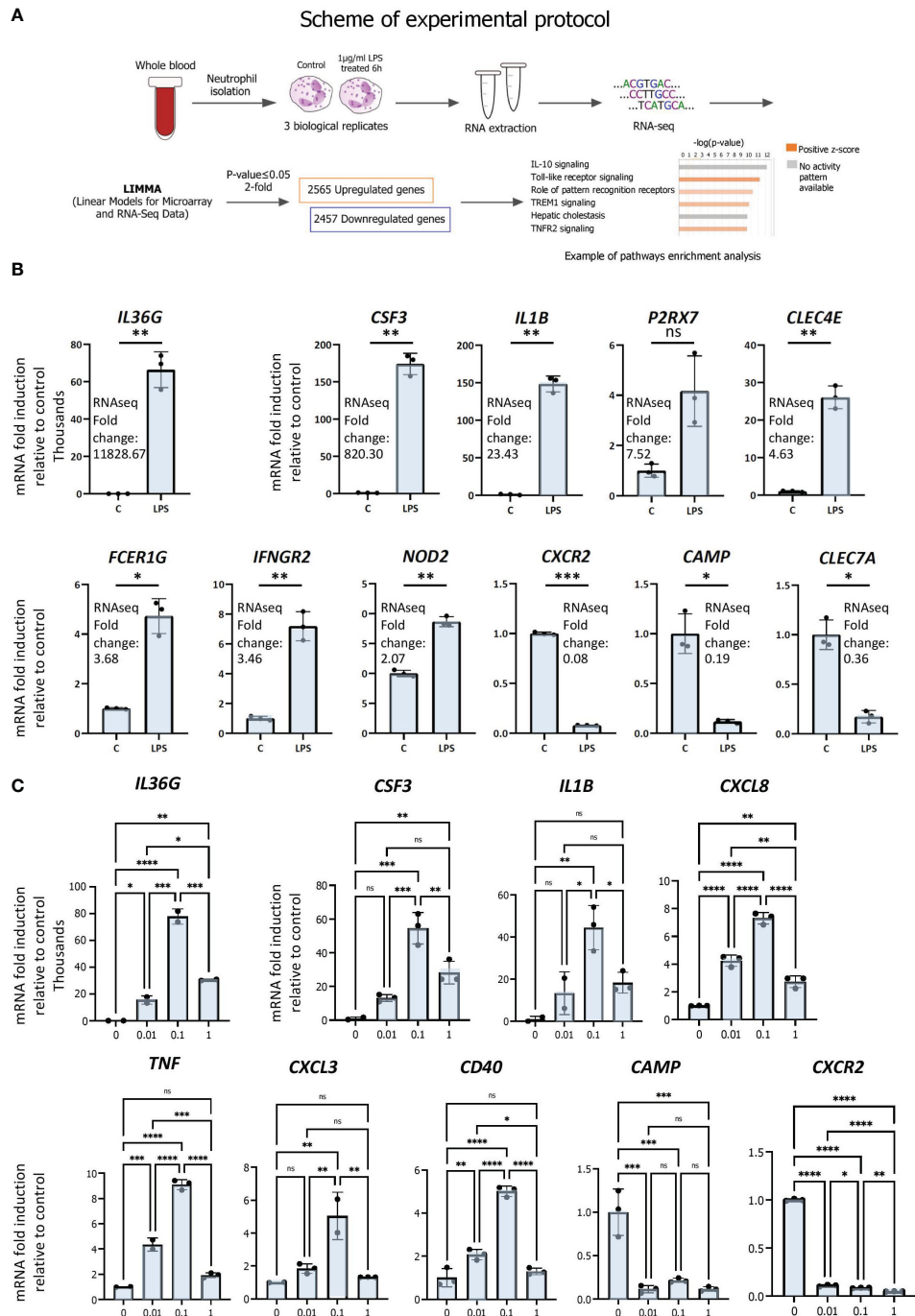


FIGURE 1 RNAseq analysis of primary human neutrophils. **(A)** Schematic representation of workflow for RNAseq analysis of LPS-regulated gene expression in neutrophils. **(B)** Validation of regulation by LPS of differentially expressed genes by RT/qPCR analysis. Data are representative of 2 or 3 biological replicates. * $P \leq 0.05$, ** $P \leq 0.01$, *** $P \leq 0.001$ and ns ≥ 0.05 as determined by paired Student's t-test for technical replicates of one representative sample. **(C)** Dose-response curves of LPS. Primary human neutrophils were treated for 6h with 0 to 1 µg of LPS per ml and RT/qPCR was subsequently performed. Graphics are mean \pm SD from 3 technical replicates and data are representative of 2 or 3 biological replicates. * $P \leq 0.05$, ** $P \leq 0.01$, *** $P \leq 0.001$, **** $P \leq 0.0001$ and ns ≥ 0.05 as determined by one-way ANOVAs followed by Tukey's *post hoc* test for multiple comparisons.

Meta-analysis of LPS-challenged neutrophils and identification of a forkhead box transcription factor network

To compare our data with those of other gene expression studies of LPS-stimulated human and mouse neutrophils, we conducted a

meta-analysis of our RNAseq data and other available microarray and RNAseq expression profiles. Datasets from the Gene Expression Omnibus (GEO) public repository with available raw data were included, which produced 14 human microarray studies and 2 mouse RNAseq expression profiles (Table S1). Differential gene expression analysis was carried out using the same pipeline to

ensure that results were comparable (see Methods); the Linear Models for Microarray Data (LIMMA) Bioconductor package was used, as it performs well in different settings for microarray and RNAseq experiments (34). Quality control (QC) of RNAseq and microarray datasets was determined, and Figures S3, S4 provide examples of QC criteria for human and mouse expression profiles (see also materials and methods for details). We included profiles generated with neutrophils stimulated *in vitro* with different concentrations of LPS over time periods ranging from 1 to 16h (see Table S1 for details). *In vivo* profiles were derived from patients administered an intravenous bolus injection of LPS for 1-6h (human endotoxemia model), followed by isolation of cells from serum, either as total neutrophil populations or as subpopulations sorted for CD16 and CD62L expression levels, markers of neutrophil maturity (21, 24, 25). Generally, the *in vivo* profiles gave rise to much smaller and more heterogeneous datasets. Expression patterns of the sorted subpopulations and total neutrophils were essentially completely different (Figure S2), with the exception of partial overlap between total and CD16^{dim}/CD62L^{bright} cells, a subset that arises rapidly upon experimental human endotoxemia (25, 35).

Our study represents the first RNAseq transcriptional analysis of LPS-stimulated human neutrophils and produced the largest number of up- and downregulated genes. Venn diagrams depicting up- and downregulated genes at least 2-fold in our data and other human *in vitro* and *in vivo* expression profiles from LPS-stimulated neutrophils revealed substantial overlap with other *in vitro* datasets (Figures 2A, S1). Our data was strongly enriched in genes regulated in gene transcription. It also showed more enrichment than others for diseases and functions, such as chemotaxis, cell binding, viral infection and apoptosis, largely because of the greater number of regulated genes identified (Figure 2B). Notably, the canonical pathways regulated as well as upstream regulators identified in our profile were most similar to those of the smaller study of Khaenam et al. (26), who also treated neutrophils *in vitro* for 6h with LPS (Figures 2C, 3A). There was substantially less overlap in our regulated gene sets with those identified in *in vivo* studies, all of which generated considerably smaller datasets (21, 24, 25).

As genes implicated in regulation of transcription were enriched in our dataset, we were interested in determining the transcription networks induced downstream of LPS stimulation. In our study, the most strongly enriched network was originally identified as being driven by the forkhead box transcription factor FOXL2 (Figure 3B) (36). Notably, the Z-score for the network is greater than those driven by RELA and STAT3, previously identified as regulators of LPS-induced inflammation in neutrophils (16, 17). Moreover, the FOXL2 network is conserved among other human and mouse *in vitro* LPS-stimulated neutrophil datasets (Figures 3C, D). In contrast, it is not upregulated in two neutrophil subsets derived from cells exposed to LPS *in vivo* (Figure 3C). However, the vast majority of upstream regulators appear downregulated in these datasets (Figure 3A). In our data, 20 of the 22 genes in the network were induced, consistent with activation of a transactivator (Figure 4A). The network is based on the identification of transcription targets of FOXL2 in a human ovarian granulosa-like tumour (KGN) cell line (36). Nonetheless, numerous genes in the network encode proteins implicated in neutrophil

function, and among those are chemokines, such as *CCL20* and *CXCL2* (37, 38) as well as stress and inflammation-associated transcription factors, *MAFF* and *ATF3* (20, 39–42) (Figure 4A). Other genes in the network encode regulators of neutrophil survival, such as *BCL2A1* and *IER3*, respectively (43, 44) (Figure 4A). Genes implicated in other aspects of neutrophil function are also enriched. These include *ICAM1*, which promotes neutrophil adhesion and transcellular migration (45); *SOD2*, a mitochondrial enzyme capable of inducing neutrophil burst, leading to intracellular killing of pathogens (46); and *NR4A3*, an orphan nuclear receptor that boosts neutrophil numbers and survival (47) (Figure 4A). We validated increased expression of several of these genes by RT/qPCR analysis in neutrophils challenged with LPS (Figure 4B). Collectively, these findings suggest that the transcription network influences several aspects of neutrophil function and survival.

Induction of FOXP1 and FOXP4 expression in LPS-exposed neutrophils

Although *FOXL2* is not expressed in our dataset, forkhead box transcription factors *FOXP1* and *FOXP4* are expressed and induced by LPS in primary human neutrophils (48) (Figure 5A). Given that FOX transcription factors have highly conserved DNA binding domains, we hypothesized that FOXP1 and/or FOXP4, rather than FOXL2, drive expression of the network of genes in neutrophils (27). Previous studies revealed the importance of FOXP1 and FOXP4 in lymphocyte development and effector cytokine production, respectively (50–53), and FOXP1 regulates monocyte differentiation (54). We compared FOXP1 motifs from the JASPAR 2020 database with those of FOXL2, as determined by Carles et al. (49) (Figure 5B), which revealed that FOXP1 and FOXL2 recognize essentially identical sequence “TGTAACA” motifs, with the exception of the variable 5' end of the sequence (Figure 5B). (Note that FOXP4 motifs are not identified in the JASPAR database). We confirmed increased gene and protein expression of the two proteins in LPS-stimulated neutrophils by RT/qPCR and Western blot analyses (Figures 5C, D). Subsequently, FOXP1/4 ChIPseq peaks were identified within 14 of the 20 genes in the FOXL2 network using published ChIPseq studies and datasets from the ENCODE consortium (55, 56) (Figure 5E, Table S2). To find sequence motifs enriched in enhancers, we extracted their sequence from the hg19 or hg38 genome and used this as input for the Transcription factor Affinity Prediction (TRAP) web tool (<http://trap.molgen.mpg.de/cgi-bin/home.cgi>) (see Methods and Materials for details) (S2 File). The frequency of the FOXP1/P4 peaks in the neutrophil network genes was remarkable given that the ChIPseq studies were performed in the DLD1 colon and HepG2 liver cancer cell lines, as well as in embryonic stem cells (55, 56) (Table S2). FOX protein consensus GTAAACA or near-consensus motifs were present at multiple binding sites in 8 of the 14 network genes containing ChIPseq peaks (see Figure 5E). By comparison, the van Bostel et al. study (56) identified TGTTTAC, the reverse complement sequence of GTAAACA, motifs in the vicinity of 30% of FOXP1 ChIPseq peaks. Notably, genes that contain the FOX protein motifs

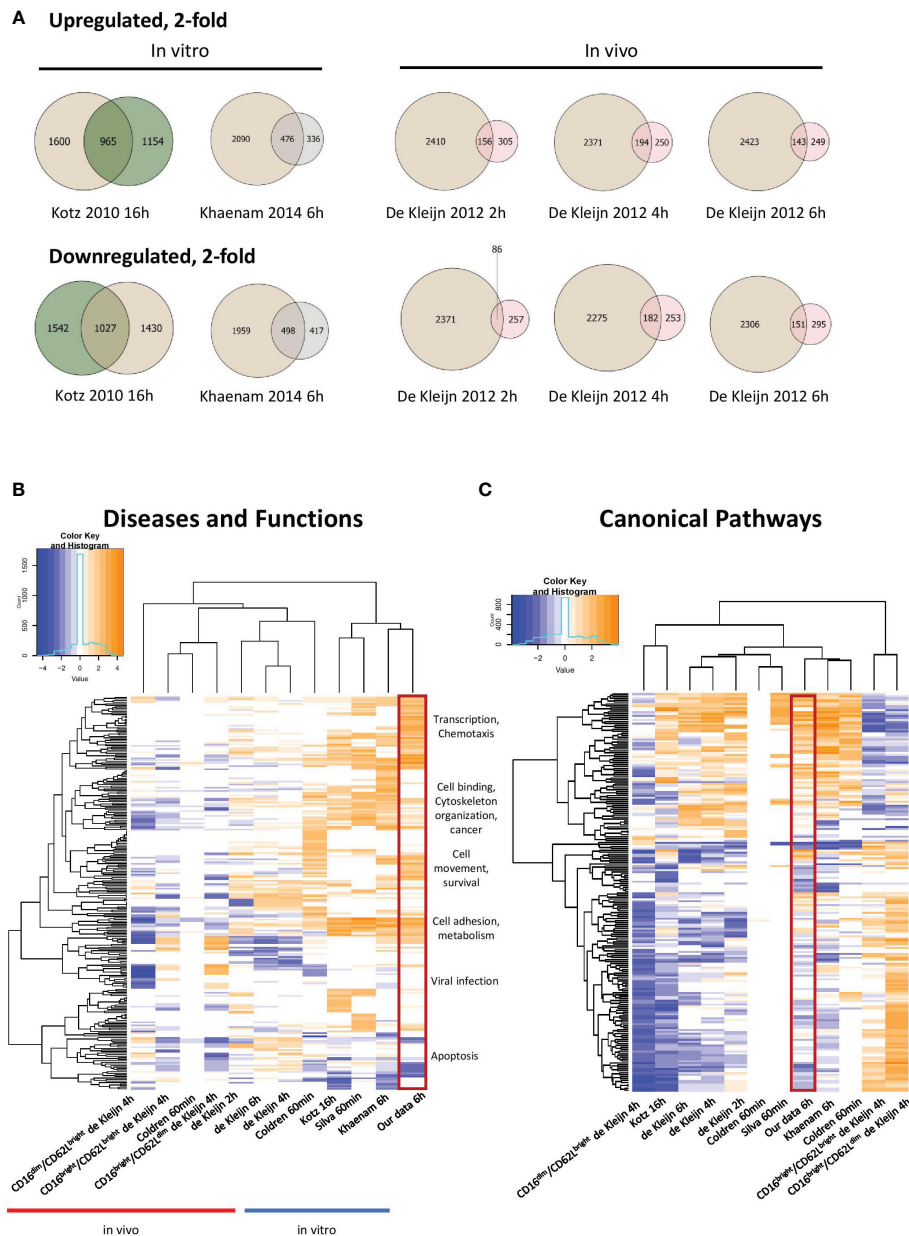


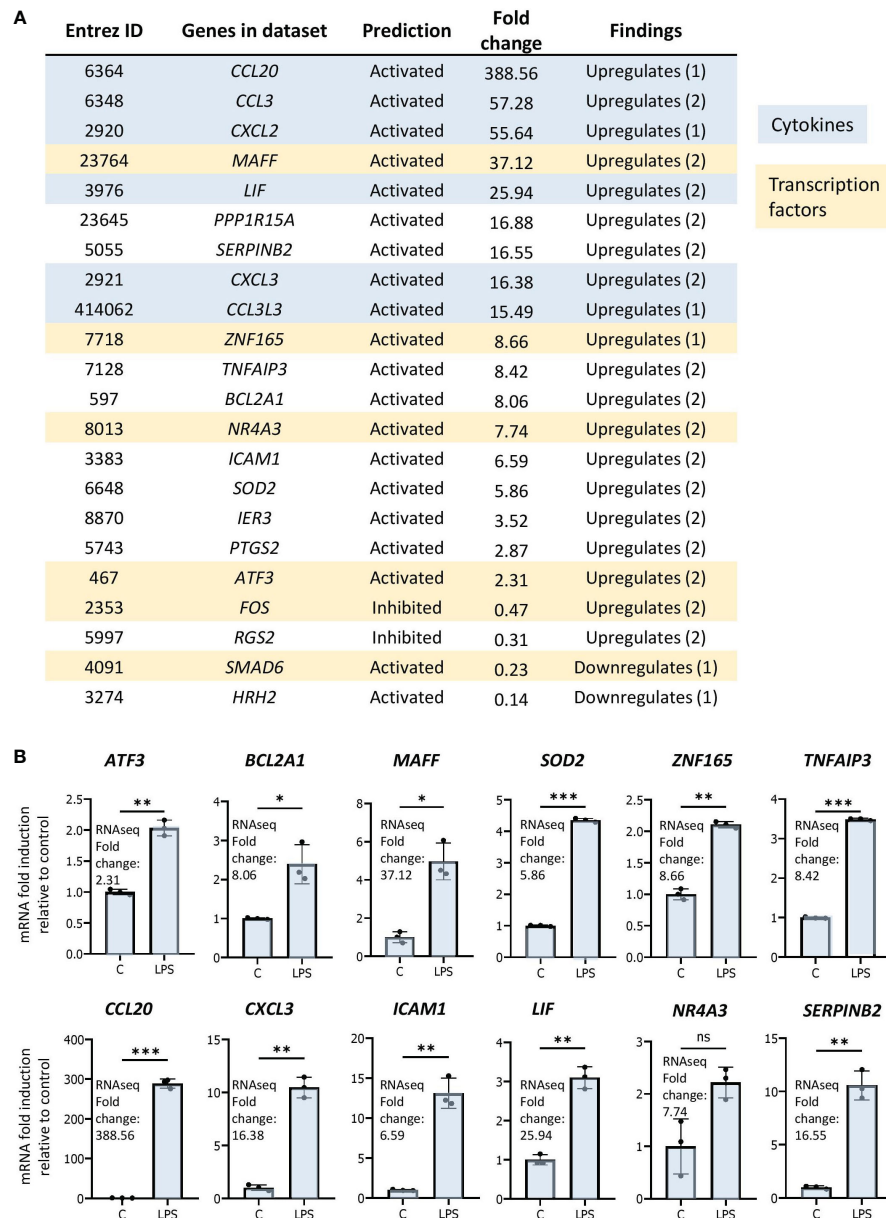
FIGURE 2

Meta-analysis of our data and other previously published LPS-treated neutrophil expression profiles. (A) Venn diagrams illustrating partial overlap in genes regulated 2-fold in our dataset and other *in vitro* and *in vivo* datasets from LPS-stimulated neutrophils. Tan colour represents our 6h data and green, pink or grey colours represent previously published datasets, as indicated in the figure. Enriched diseases and biological functions (B) and canonical pathways (C) of genes in our dataset compared to other datasets from LPS-stimulated neutrophils ($-\log p \text{ value} \leq 1.3$). Categories with a predicted activation state (positive Z-score) are labeled in orange while those with a predicted inhibition state (negative Z-score) are indicated in blue. Hierarchical clustering is shown to reveal similarly enriched datasets to our data. Our data is enclosed in the red rectangle.

included inflammation-induced transcription factors MAFF, ATF3, and ZNF165 and those encoding several cytokines (Figure 5E).

To further probe whether the FOXP1/P4 ChIP binding sites may be active in neutrophils, we identified regions of histone marks in neutrophils corresponding to enhancers (regions of H3K4 trimethylation and H3K27 acetylation) from datasets from the ENCODE consortium (Figures 6A, S6; Table S2). Notably, the binding sites containing motifs do not overlap areas of H3K27 or H3K9 trimethylation (Figures 6A, S6), which are histone marks indicative of transcriptionally repressed regions. Furthermore, we found that the promoter-proximal FOXP1/P4 binding sites overlap

with RNA polymerase II binding profiles in neutrophils, as illustrated in the UCSC browser image for the *ZNF165* locus (Figure S6). Two clusters of FOXP1/4 binding sites are present in the vicinity of the *MAFF* gene; one at approximately 14 kb upstream from the transcription start site (TSS), and another in an intronic region of the gene (~700 bp from the TSS) (Figures 6A, S6). Furthermore, a promoter-proximal FOXP1 binding site at 221 bp downstream from the TSS containing a FOX protein motif is present in the *ZNF165* gene (Figure S6). Taken together, these results strongly suggest that, in LPS-treated cells, putative FOXP1 and FOXP4 binding sites are present in regions corresponding to neutrophil enhancers.



either of the two proteins (Figure 7A). FOXP1 and FOXP4 expression was observed in cells transiently transfected with corresponding expression vectors (Figure 7A). ChIP assays were performed to analyse binding of the two proteins to multiple binding sites identified above. FOXP4 binding was observed to all sites (Figure 7B). Remarkably, robust binding of FOXP1 by ChIP was also observed to all sites (Figure S7C), with the strongest signals at sites adjacent to the *ATF3* and *SOD2* genes. Importantly, we also observed a general increase in mRNA expression of multiple network genes in transfected HEK293 cells (Figure 7C). Taken together, these data show that expression of network genes is induced under conditions of elevated forkhead box transcription factor expression.

We next investigated whether induction of the forkhead box protein network is observed in neutrophils stimulated with inflammatory agents other than LPS. The GEO repository was used to search for expression profiles of human neutrophils challenged with inflammatory signals, which generated 4 microarray datasets (see Table S3 for details) (23, 47, 57, 58). They included neutrophils challenged with the protein kinase A agonist pair 8-AHA-cAMP and N6-MB-cAMP (N6/8-AHA) and cytokines GM-CSF and interferon-gamma (IFN- γ) over time periods ranging from 3–24h (Table S3) (23, 47). Analysis of these datasets revealed that the FOX protein network was enriched in all profiles with a high Z-score (Figure 8).

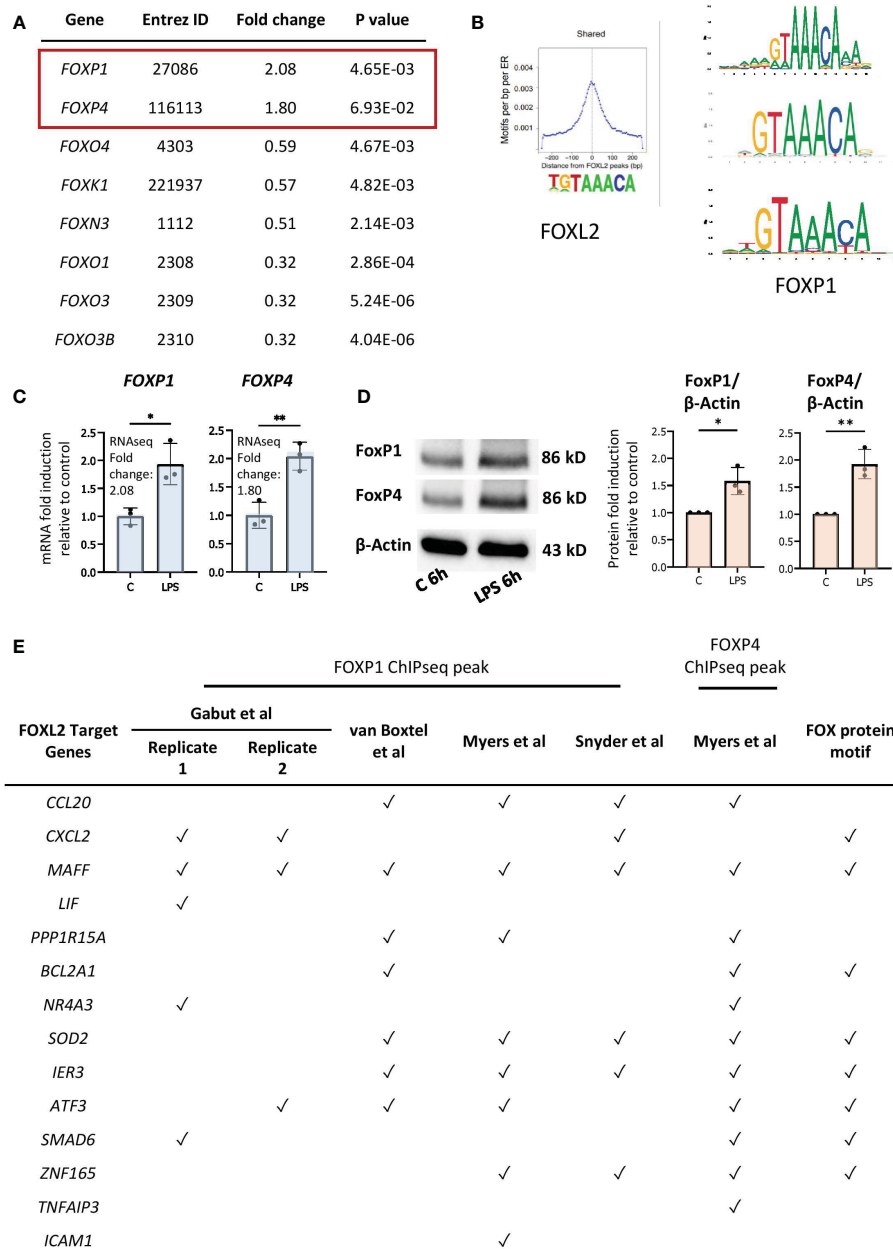


FIGURE 5

FOXP1 and FOXP4 binding sites are present in regulatory regions of network genes. (A) Up- and downregulated genes by LPS encoding FOX transcription factors in our RNAseq data. (B) Conserved motifs (sequence logos) of FOXL2 (left, retrieved from Carles et al. (49)) and FOXP1 (right, retrieved from the JASPAR 2020 database). (C) RT/qPCR analysis of LPS-regulated expression of genes encoding the FOX transcription factors, FOXP1 and FOXP4. Data representative of 2 or 3 biological samples. Graphics are mean \pm SD from 3 technical replicates from a representative sample and paired, two-tailed t-test (Student's t-test) was used (* $P \leq 0.05$ and ** $P \leq 0.01$). (D) Western analysis of FOXP1 and FOXP4 protein expression in vehicle- or LPS-treated neutrophils, as indicated. Blots show the band representing the full-length protein. Data representative of 3 biological replicates. Quantification shown on right. Graphics are mean \pm SD from 3 biological replicates and unpaired, two-tailed t-test was used (* $P \leq 0.05$ and ** $P \leq 0.01$). (E) Presence (marked by a tick) or absence of FOXP1 and/or FOXP4 ChIPseq peak(s) and FOX protein motifs within the network genes in different FOXP1 or FOXP4 ChIPseq datasets performed in various cell types.

Discussion

To date, analysis of transcriptional changes occurring in neutrophils challenged with LPS has revealed activation of NF- κ B and STAT3 transcription factors (16, 17) as well as increased pro-inflammatory cytokine expression (18–26). Additional research into such changes provides insight into novel signaling pathways and transcriptional responses driving in neutrophil immune responses

under (patho)physiological conditions. In this study, we performed the first large scale RNAseq profile to probe the human neutrophil transcriptomic responses to LPS and other inflammatory agents. Bioinformatic analysis of this data showed that treatment with LPS robustly induced a transcriptional network, initially identified as being regulated by the forkhead transcription factor FOXL2 in other cell types. However, the network is relevant to neutrophil function as it is highly enriched in genes encoding proinflammatory

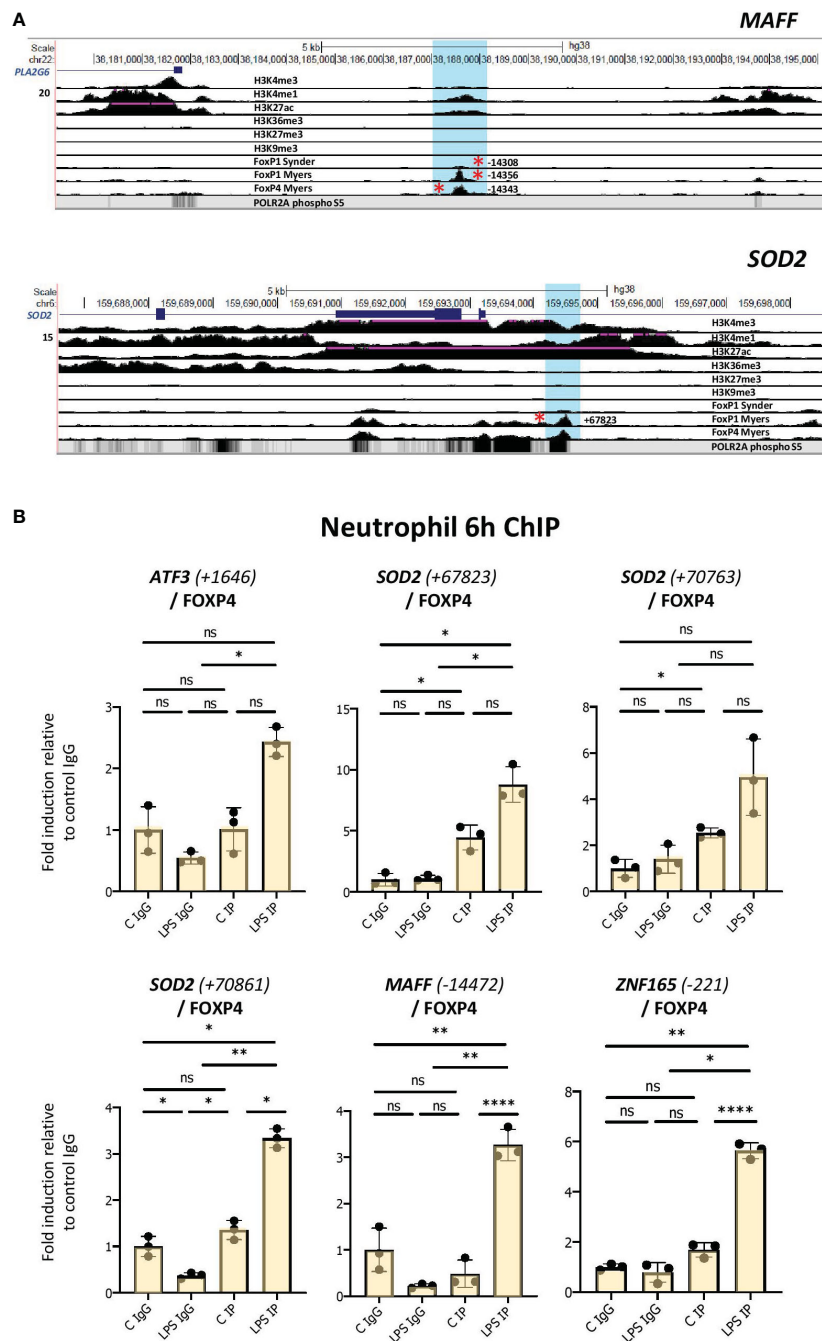


FIGURE 6
Enhanced binding of FOXP4 to network gene motifs as assessed by ChIP assay in LPS-challenged neutrophils. **(A)** UCSC browser images showing FOXP1 and FOXP4 ChIPseq tracks at MAFF and SOD2 loci. The areas surrounding the FOXP1/FOXP4 binding sites up and downstream (regions highlighted in blue) are shown. Red asterisks represent ChIPseq peaks that contain FOX protein motifs. Binding sites correspond to regions of enhancer function in neutrophils. **(B)** Analysis of the association of FOXP4 with up- and downstream regulatory regions of ATF3, SOD2, MAFF and ZNF165 by ChIP assay in neutrophils treated with or without LPS for 6h. Data representative of at least 3 biological replicates. Graphics are mean \pm SD from 3 technical replicates from a representative sample. * $P \leq 0.05$, ** $P \leq 0.01$, **** $P \leq 0.0001$ and ns ≥ 0.05 as assessed by one-way ANOVAs followed by Tukey's *post hoc* test for multiple comparisons. ChIP values are normalized to input for each condition and expressed as a fold relative to non-specific IgG control. IP represents the protein-specific antibody, FOXP4.

cytokines and transcription factors implicated in inflammatory and stress responses. Importantly, the network includes several genes encoding transcription factors such as ATF3 and MAFF, which have been implicated in cellular responses to stress and inflammatory signals (20, 39–42), as well as that encoding the orphan nuclear receptor NR4A3, whose expression controls

neutrophil numbers and survival (47). The network thus controls a cascade of transcriptional events in response to LPS.

While FOXL2 was not expressed in our RNAseq dataset, forkhead box transcription factors FOXP1 and FOXP4 were expressed and induced by exposure to LPS. Several lines of evidence indicate that FOXP4 can functionally replace FOXL2 in neutrophils. These include

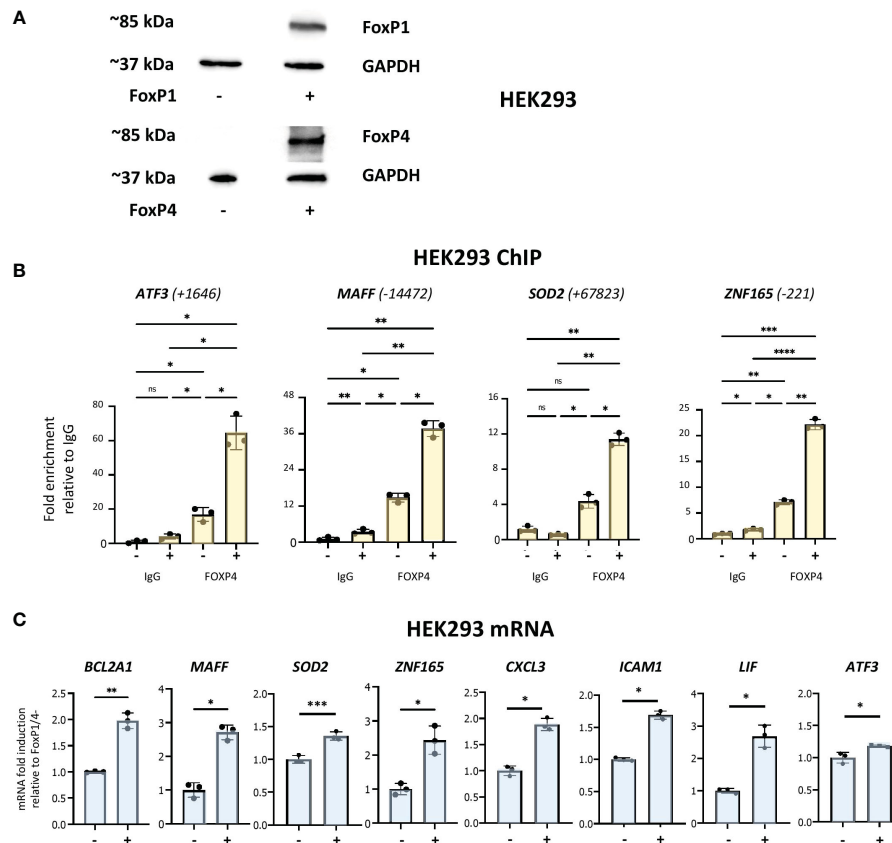


FIGURE 7

Analysis of forkhead box protein DNA-binding and gene regulation in HEK293 cells. (A) Western analysis of FOXP1 and FOXP4 protein expression in HEK293 cells transfected with or without FOXP1 and FOXP4 expression vectors, as indicated. (B) Analysis of the association of FOXP4 with up- and downstream regulatory regions of ATF3, MAFF, SOD2 and ZNF165 by ChIP assay in HEK293 cells transfected with and without FOXP1 and FOXP4 expression vectors. Data representative of 2 or 3 biological replicates. Graphics are mean \pm SD from 3 technical replicates from a representative sample and paired one-way ANOVAs followed by Tukey's *post hoc* test for multiple comparisons were used (* $P \leq 0.05$, ** $P \leq 0.01$, *** $P \leq 0.001$, **** $P \leq 0.0001$ and ns ≥ 0.05). ChIP values are normalized to input for each condition and expressed as a fold relative to non-specific IgG control. (C) RT/qPCR analysis of FOXP1/4 network genes in HEK293 transfected with and without FOXP1 and FOXP4 expression vectors. Data representative of 2 or 3 biological replicates. Graphics are mean \pm SD from 3 technical replicates from a representative sample and paired, two-tailed t-test (Student's t-test) was used (* $P \leq 0.05$, ** $P \leq 0.01$, *** $P \leq 0.001$, **** $P \leq 0.0001$ and ns ≥ 0.05).

Study	FOXL2 network activation Z-score	Number of genes 2-fold
Our data 6h	3.75	2565 up 2457 down
Wolf 6h	3.44	1171 up 650 down
Gonzalez-Cotto 8h permissive for TREML4	3.14	2413 up 4053 down
Gonzalez-Cotto 8h non-permissive for TREML4	2.99	2461 up 3936 down
Roux 4h	3.31	1750 up 869 down
Aznaourova 4h	4.21	1583 up 2021 down

FIGURE 8

FOX protein network is induced by LPS in neutrophils in response to other inflammatory signals. Lists of other datasets of human neutrophils stimulated with various human inflammatory signals. Their associated FOX network activation Z-scores and number of 2-fold regulated genes are shown as well.

the fact that members of the forkhead box transcription family recognize essentially identical DNA motifs; all FOX transcription factors have a conserved DNA binding domain and bind to essentially identical GTAAACA motifs (27, 49). Moreover, FOXP1/4 binding sites are present in network genes identified in ChIPseq studies performed in heterogeneous cell types, but located in regions that correspond to transcriptional enhancers in neutrophils. Further bioinformatics analysis revealed that the genes in the network were also regulated in neutrophils exposed to other inflammatory signals.

We performed ChIP assays on multiple isolates of primary human neutrophils and observed enhanced LPS-dependent binding of FOXP4 to several motifs adjacent to network genes. While we did find some evidence for LPS-induced FOXP1 binding in one neutrophil isolate, this finding was not generally reproducible. Studies in transiently transfected HEK293 cells showed that both FOXP1 and FOXP4 can recognize multiple motifs in network genes. The binding of FOXP1 to these motifs in HEK293 cells may be a function of its elevated expression under conditions of transient transfection. However, collectively our data suggest that we cannot rule out the possibility that FOXP1 may contribute to network gene transcription if sufficiently induced in neutrophils. Moreover, the data

in HEK293 cells showed that forkhead box transcription factor expression can induce transcription of multiple network genes.

Meta-analysis of our RNAseq data and other available comparable expression profiles revealed that canonical pathways, diseases and functions, and upstream regulators identified in other *in vitro* profiles clustered closer to our data than those derived from neutrophils exposed to LPS *in vivo*. A high activation Z-score was observed for the FOXL2 transcriptional network in all *in vitro* datasets, which is remarkable given that the meta-analysis included expression profiles performed using different platforms, and with neutrophils exposed to LPS for varying times and at different concentrations. However, the network displayed a negative Z-score for two neutrophil subpopulations acquired from cells stimulated with LPS *in vivo* (25). This may be due partly to cell sorting by FACS performed on the cells treated *in vivo*, which may perturb gene expression profiles (59). The discrepancies may also be explained by the method in which neutrophils were treated with LPS. *In vitro* neutrophil studies consist of isolating cells from human whole blood (21–23, 26). In contrast, in *in vivo* experiments, a human endotoxemia model (intravenous administration of an endotoxin solution) was employed (21, 24, 25). There is a limitation to this model as it produces a low-grade acute systemic inflammatory state and does not completely recapitulate chronic inflammation present in inflammatory diseases (60). The LPS dose *in vivo* required to stimulate, for example, sepsis (an acute inflammatory response to infection in which neutrophil function is dysregulated) is unsafe and ethically unacceptable in human studies (61). Moreover, the dynamic alterations in cytokine levels noted after LPS injection are substantially different from the more sustained levels observed in critically ill patients (61) and *ex vivo* experiments (62). Finally, the single-exposure human endotoxemia model cannot capture sustained innate immune activation that may occur with chronic exposure to inflammatory agents (60).

In addition to LPS, the network identified here may be regulated by other upstream regulators or stimuli. We found that the network was induced in response to other neutrophil inflammatory agents, such as the protein kinase A agonist pair N6/8-AHA and cytokines GM-CSF and IFN- γ . In addition, bioinformatic analysis of gene expression in neutrophils treated with two different strains of bacteria revealed a high activation Z-score for the network. Germline deletion of FOXP1 or FOXP4 leads to embryonic lethality in mice due to cardiac defects (48, 63). Other studies have investigated the role of the two proteins in T and B lymphocytes using conditionally targeted strains in rodents (50–53). Feng et al. crossed floxed FOXP1 mice with Cd4^{Cre} transgenic mice (50, 51). These conditional knockout studies found that FOXP4 and FOXP1 are implicated in the regulation of B and T cell development and cytokine production. Additionally, FOXP1 is expressed in untreated and retinoic acid-induced differentiated HL-60 cells; its expression was inhibited in phorbol ester-induced HL60 monocytic differentiation but not in retinoic acid-induced granulocytic differentiation (54). Collectively, therefore, our findings and evidence from their roles in regulation of other immune cell types suggest that FOXP1 and/or 4 may play key roles in neutrophil biological functions. Conditional knockouts of FOXP1 and/or FOXP4 would be a future avenue of study to better understand the roles of the two proteins in neutrophil

differentiation and function. In conclusion, our study identifies a novel transcription network induced by forkhead box transcription factors in neutrophils exposed to inflammatory stimuli. Our findings lay the foundation for additional investigations into the roles of FOXP4 and FOXP1 in neutrophil biology. Further research using appropriate animal models are required to assess their function and the role of the network in neutrophil-associated inflammatory diseases, such as rheumatoid arthritis and cancer.

Materials and methods

Human neutrophil isolation and treatment

Whole blood from consenting healthy donors was provided by Dr. Jack Antel (McGill) through C-Big under McGill University Health Centre REB ethics #2021-6588. Primary human neutrophils were isolated from blood by negative selection using the EasySepTM Direct Human Neutrophil Isolation Kit (STEMCELL) according to the manufacturer's instructions. Purity of neutrophils was determined by flow cytometry by quantifying markers of various cell populations found in blood, notably CD45 (hematopoietic cells with the exception of erythrocytes and platelets), CD16 (natural killer cells, neutrophils and macrophages) and CD66b (granulocytes). Cells were counted by an automatic cell counter (Bio-Rad) and adjusted to a concentration in between 5×10^5 and 1×10^6 cells/ml. Neutrophils were resuspended in tissue culture medium, which consisted of RPMI 1640, 1X with L-glutamine, sodium pyruvate & 25mM HEPES (350-006-CL, Wisent) supplemented with 10% fetal bovine serum and penicillin/streptomycin (0503, ScienCell). Cells were subsequently treated with 1 μ g/mL LPS (L3012-5MG, Sigma-Aldrich) or vehicle (dimethyl sulfoxide) for 6 hours. By annexin V/propidium iodide staining, we showed that after 6h neutrophils were mostly viable (Figure S8).

Data collection

We mined the PubMed database for microarray and RNAseq expression profiling. We used the following key words and their combinations: “Neutrophil, LPS, lipopolysaccharide, microarray, RNAseq, gene expression dataset”. Furthermore, the Gene Expression Omnibus (GEO) public repository was used to search for studies using the keywords “lipopolysaccharide AND neutrophil.” Gene expression studies investigating the effects of lipopolysaccharide on neutrophils, for which the raw data were available, were included. We extracted the following information from each identified study: publication reference, GEO accession number, dose and time of LPS treatment, platform, and number of biological replicates (Table S1). The analysis excluded studies in LPS knockout mice.

RNA sequencing

Total RNA from triplicate isolates of LPS- and vehicle-treated neutrophils was extracted using FavorPrep Blood/Cultured Cell Total

RNA Mini Kit (FABRK 001, Favorgen) as per the manufacturer's instructions. Biological replicates were generated from 3 independent neutrophil isolates. Only RNA samples with OD 260/280 ratio greater than 1.7 and a RNA integrity number (RIN) > 7 were kept for downstream analysis. These samples were submitted to McGill University and Genome Quebec Innovation Centre for paired-end sequencing at 50M reads on an Illumina NovaSeq 6000 S2 PE100 sequencer. Library preparation were conducted using the Illumina mRNASeq stranded library kit and the adapter used was NEBNext dual. 3 and 2 replicates for control and LPS-treated conditions, respectively, were of high enough quality for downstream analysis as determined by QC reports performed by Genome Quebec. The quality of sequence reads obtained for each sequence read was confirmed using FastQC. The measure of poor quality used was the Phred score, which is logarithmically related to the probability of errors in base calling (64). For all RNAseq datasets, the Phred offset quality score was greater than 30 and the minimum fragment size for alignment was set to 50. Low-quality bases were trimmed from read extremities using default settings in Trimmomatic (65), and quality was re-assessed using FastQC. Reads were then mapped to the human GRCh38 genome assembly using HISAT2 (66). Gene expression was quantified by counting the number of uniquely mapped reads with StringTie (67) using default parameters. Normalization and differential gene expression analysis was conducted using the DESeq2 Bioconductor package (68). Genes with changes in expression $\geq |2|$ and adjusted p-values (≤ 0.05) were considered significant. Principal component analysis (PCA) was performed using the built-in R function, `prcomp`, and visualized with the `ggplot` package (Figure S3). Enrichment analyses of upstream regulators, canonical pathways, as well as diseases and functions on differentially expressed genes were performed using QIAGEN's Ingenuity Pathway Analysis software (IPA[®], QIAGEN Redwood City, www.qiagen.com/ingenuity). The raw and processed RNAseq data are deposited in GEO under the accession number GSE221866.

Flow cytometry

Adherent neutrophils were detached by gently pipetting the tissue culture dishes up and down. Adherent and suspension cells were centrifuged at 500 rcf for 10 min, and washed twice with ice-cold PBS. The supernatant was subsequently removed. We resuspended the cells in FACS buffer (0.5-1% BSA in PBS) at a concentration of 1×10^6 cells/ml and blocked the cells with human FcR binding inhibitor (14-9161-73, eBioscience). To determine neutrophil purity, 2 μ g of anti-human PerCP/Cy5.5-CD66b (305107, BioLegend), PE-CD16 (302007, BioLegend), and PE/Cy7-CD45 (103113, BioLegend) antibodies were added and incubated for 30 min at room temperature in the dark. Viability was assessed using the Vybrant Apoptosis Assay kit (V13242, Molecular Probes). Cells were washed and either cross-linked in 2% paraformaldehyde or immediately analyzed by flow cytometry for purity and viability experiments, respectively. A BD-LSRFortessa analyzer was employed for flow cytometry acquisition and at least 10 000 cells/sample were monitored. The FlowJo software (TreeStar Inc.) was subsequently used for data analysis.

Meta-analysis of gene expression profiles

Analyses of gene expression profiles was performed using the R statistical package. The `oligo` package was employed to receive signal intensities from CEL files of Affymetrix microarrays; data was normalized and summarized using the Robust Multi-Array Average method, a component of the `oligo` package. Using Illumina's `BeadStudio`, Illumina raw input was summarized. The `LIMMA` package in R was employed to normalize Illumina, Agilent, Nimblegen, and custom arrays. RNAseq raw files (SRA) were downloaded and transformed to reads in fastq format by the `fastq-dump` function in the `sra` toolkit suite from NCBI. A genome index was constructed derived from human/mouse genomes, supplied by Guillimin, Calcul Quebec high-performance computing cluster at McGill University, using the `Rsubread` package. The latter was also used to align RNAseq reads to retrieve read counts based on the "seed-and-vote" paradigm. The ensuing data was arranged for downstream analysis using the package `EdgeR`. For assessing differential gene expression for microarray and RNAseq data, the `LIMMA` package was employed. Differentially-expressed genes were 2-fold regulated and p value ≤ 0.05 was used as the threshold for significance. The `biomaRt` package, an interface to the BioMart databases at Ensembl, was used for annotation, including human orthologs for mouse genes.

Quality control criteria

Each RNAseq dataset had similar total number of RNAseq reads sequenced for each condition and total GC content. The Phred offset quality score was greater than 30 for all RNAseq datasets and the minimum fragment size for alignment was set to 50. These settings yielded 70% to 85% of reads aligning to a gene using the `Rsubread` and `EdgeR` packages in R. We filtered out genes with low read counts and included genes with counts of 10 or more for at least 1 treatment group (in all replicates) for downstream analysis. To validate similarity between replicates in each treatment group, we performed a principal components analysis (Figure S3). For Illumina microarray platforms, the probe summary files, which comprised the control probes, were exported from Illumina's `GenomeStudio` without background correction or normalization. Raw files from the remaining microarray datasets were analyzed in R using the `GEOquery`, `oligo` and `LIMMA` packages. To determine potential outliers in microarray datasets, we visualized signal distribution of the raw and normalized data using box plots (Figure S4). Samples in all datasets seemed comparable following background correction and normalization.

Bioinformatics analysis

Venn diagrams were generated with the `VennDiagram` package in R. Enriched canonical pathways, upstream regulators, biological diseases and functions as well as the FOXP1/4 upstream transcriptional network were identified using QIAGEN's Ingenuity Pathway Analysis software (IPA[®], QIAGEN Redwood City, www.qiagen.com/ingenuity).

qiagen.com/ingenuity). Heatmaps with hierarchical clustering were constructed using the `heatmap.2` package in R. Peaks from FOXP1/4 ChIPseq studies and datasets from the ENCODE consortium were aligned with the human genome (build hg19 or hg39) using the UCSC Genome Browser (<http://genome.ucsc.edu/cgi-bin/hgGateway>). FOXP1 or FOXP4 binding sites were considered if they were within 25kb of a gene and in regions of active (either H3K4 trimethylation and H3K27 acetylation), but not repressive (H3K27 nor H3K9 trimethylation) histone marks in neutrophils using the statistical analyses provided in each publication. To find sequence motifs enriched in enhancers in human cancer cell lines and embryonic stem cells, we extracted their sequence from the hg19 or hg38 genome and used this as input for the Transcription factor Affinity Prediction (TRAP) web tool (<http://trap.molgen.mpg.de/cgi-bin/home.cgi>) using JASPAR vertebrates as the comparison library, human promoters as the control, and Benjamini-Hochberg as the correction (69). We used a p value threshold of 0.05. This resulted in the enrichment of several consensus or near-consensus motifs (S2 File) for FOX transcription factors. Matrices used were FOXO3: MA0157.1; FOXD1: MA0031.1; FOXF2: MA0030.1, FOXA1: MA0148.1, and FOXC1: MA0032.1.

Cell culture

HEK293 cells were obtained from the American Type Culture Collection (ATCC) and cultured in DMEM (319-005-CL, Wisent) supplemented with 10% fetal bovine serum and penicillin/streptomycin.

RNA extraction, reverse transcription and qPCR

We performed RNA extraction with the FavorPrep™ Tissue Total RNA Mini Kit (FATRK 001, Favorgen) as per the manufacturer's instructions. cDNA was acquired from 100 - 500 ng of RNA using 5× All-in-One RT Mastermix (G485, abm) and diluted 5 times. Quantitative polymerase chain reaction (qPCR) was performed with BrightGreen 2×qPCR MasterMix (MasterMix-LR-XL, abm) on a Roche Applied Science LightCycler 96 machine. We normalized the expression of genes was normalized to *18S* or *ZC2HC1C*. All primers are listed in Table S4.

Western blotting and protein analysis

Primary human neutrophils and HEK293 cells were solubilized in Lysis Buffer (20 mM Tris, pH 8, 150 mM NaCl, 1% Triton X-100, 3.5 mM sodium dodecyl sulfate, 13 mM deoxycholic acid) and extracted proteins were separated on a 4% to 15% Tris/Glycine/sodium dodecyl sulfate gel (Bio Rad). For transfer and blotting, we used a standard protocol. FOXP1 (#ab16645, abcam, 1:500) and FOXP4 (#ab17726, abcam, 1:500) primary antibodies were purchased from Abcam. The antirabbit IgG HRP-linked secondary antibody was purchased from Cell Signaling Technology and used at recommended concentrations. Signals of protein bands were detected using Clarity ECL chemiluminescent substrates (Bio-Rad) and ChemiDoc Imaging System (Bio-Rad). We quantified changes in protein levels relative to

control using Image Lab software after normalization to β -actin or GAPDH (Cell Signaling Technologies), as indicated. Western blot images are representative of three biological replicates. Full western blots for FOXP1 and FOXP4 are provided in Figure S5 and correspond to the full-length FoxP1 and FoxP4 protein as described in (50, 70–73).

Chromatin immunoprecipitation assays

Cells were cross-linked with 1% formaldehyde for 15 min and were lysed with 500 μ l lysis buffer (20mM Tris HCl pH 8, 1% SDS, 50mM NaCl) containing 1x protease inhibitor cocktail (with EDTA). Chromatin samples were sheared to a length of 300-500 bp *via* sonication. Following centrifugation, supernatants were collected and 2 μ g of antibody (#ab16645 [FOXP1], #ab17726 [FOXP4], Abcam) was added to chromatin to immunoprecipitate overnight. Dynabeads Protein G (10003D, Thermofischer) was added to antibody chromatin complexes for 2h. Next, protein G bead-chromatin complexes were washed twice with dilution buffer (20mM Tris HCl pH 7.6, 1% Triton X-100, 150mM NaCl) and once with washing buffer (PBS, 0.02% Tween-20, pH 7.4), as specified by manufacturer's instructions. Proteinase K (P8107S, New England Biolabs) was added to immunoprecipitated and input chromatin; samples were then incubated at 45°C for 2h. Subsequently, chromatin was heated at 64°C for 4h for reversal of formaldehyde crosslinking. DNA fragments were purified using a PCR purification kit (FAGCK001-1, Favorgen) and were analyzed by qPCR. Antibodies used for ChIP are the same as for western blotting. Primer pairs used for ChIP assays are listed in Table S4.

Statistics

Two-tailed t-test (Student's t-test), performed using GraphPad software, was used to determine significance of results for 2 conditions. For 4 conditions, a one-way ANOVA followed by Tukey's *post hoc* test for multiple comparisons was used using GraphPad. A p value of less than or equal to 0.05 was considered significant. To denote p values, symbols were used as follows: **P \leq 0.05, ***P \leq 0.001, ****P \leq 0.0001, and ns \geq 0.05. Results from RT/qPCR, western blotting and ChIP analyses are representative of at least 3 biological replicates and one-way ANOVAs were used to determine significance. Paired tests were used for technical replicates of a representative sample and unpaired tests were used for biological replicates.

Data availability statement

The processed data from our RNAseq on LPS-stimulated human neutrophils can be found in S1 File. Enriched canonical pathways and upstream regulators of our data and other datasets of LPS-challenged neutrophils can be found in S3 and S4 files, respectively. The raw data from our RNAseq on LPS-stimulated human neutrophils presented in the study are publicly available. This data can be found here: <https://0-www-ncbi-nlm-nih-gov.brum.beds.ac.uk/geo/query/acc.cgi?acc=GSE221866> or under accession number GSE221866.

Ethics statement

The studies involving human participants were reviewed and approved by Dr. Jack Antel (McGill) through C-Big under McGill University Health Centre REB ethics #2021-6588. The patients/participants provided their written informed consent to participate in this study.

Author contributions

Wrote the paper: AI, JW. Conceived and designed the experiments: JW, AI. Performed the experiments: AI, VD, CB. Methodology of ChIP assays and HEK293 transfections: RS-T, BM. Analyzed experimental data: AI. Methodology and analysis of bioinformatics: AI, VD. Supervision: JW. All authors contributed to the article and approved the submitted version.

Funding

This work was supported by a grant from the Canadian Institutes of Health Research (CIHR PJT-180271) to JW. AI is the holder of a doctoral fellowship from the Fonds de la Recherche Québec – Santé. The funders had no role in study design, data collection and analysis, decision to publish, or preparation of the manuscript.

Acknowledgments

We are grateful to Drs. Jack Antel, Luda Diatchenko, Jörg Fritz, Jo Stratton, Jelani Clarke and Catie Futhey as well as Nicholas Kieran, Maha Zidan and blood donors for providing primary human

neutrophils. We thank the Flow Cytometry and Cell Sorting Facility at McGill, as well as Julien Leconte and Camille Stegen, for assistance with the flow cytometry experiments; the facility's infrastructure is supported by the Canada Foundation for Innovation (CFI). We are grateful to Nailya Ismailova for assistance with LPS-dose response curves.

Conflict of interest

The authors declare that the research was conducted in the absence of any commercial or financial relationships that could be construed as a potential conflict of interest.

Publisher's note

All claims expressed in this article are solely those of the authors and do not necessarily represent those of their affiliated organizations, or those of the publisher, the editors and the reviewers. Any product that may be evaluated in this article, or claim that may be made by its manufacturer, is not guaranteed or endorsed by the publisher.

Supplementary material

The Supplementary Material for this article can be found online at: <https://www.frontiersin.org/articles/10.3389/fimmu.2023.1123344/full#supplementary-material>

References

- Burn GL, Foti A, Marsman G, Patel DF, Zychlinsky A. The neutrophil. *Immunity* (2021) 54(7):1377–91. doi: 10.1016/j.immuni.2021.06.006
- Filep JG, Ariel A. Neutrophil heterogeneity and fate in inflamed tissues: implications for the resolution of inflammation. *Am J Physiol Cell Physiol* (2020) 319(3):C510–c32. doi: 10.1152/ajpcell.00181.2020
- Herrero-Cervera A, Soehnlein O, Kenne E. Neutrophils in chronic inflammatory diseases. *Cell Mol Immunol* (2022) 19(2):177–91. doi: 10.1038/s41423-021-00832-3
- Margraf A, Lowell CA, Zarbock A. Neutrophils in acute inflammation: current concepts and translational implications. *Blood* (2022) 139(14):2130–44. doi: 10.1182/blood.2021012295
- Nakabo S, Romo-Tena J, Kaplan MJ. Neutrophils as drivers of immune dysregulation in autoimmune diseases with skin manifestations. *J Invest Dermatol* (2022) 142(3, Part B):823–33. doi: 10.1016/j.jid.2021.04.014
- Wigerblad G, Kaplan MJ. Neutrophil extracellular traps in systemic autoimmune and autoinflammatory diseases. *Nat Rev Immunol* (2022), 1–15. doi: 10.1038/s41577-022-00787-0
- Nathan C. Neutrophils and COVID-19: Nots, NETs, and knots. *J Exp Med* (2020) 217(9):1–3. doi: 10.1084/jem.20201439
- Tomar B, Anders HJ, Desai J, Mulay SR. Neutrophils and neutrophil extracellular traps drive necroinflammation in COVID-19. *Cells* (2020) 9(6):1–8. doi: 10.3390/cells9061383
- Wang J, Li Q, Yin Y, Zhang Y, Cao Y, Lin X, et al. Excessive neutrophils and neutrophil extracellular traps in COVID-19. *Front Immunol* (2020) 11:2063. doi: 10.3389/fimmu.2020.02063
- Quail DF, Amulic B, Aziz M, Barnes BJ, Eruslanov E, Fridlender ZG, et al. Neutrophil phenotypes and functions in cancer: A consensus statement. *J Exp Med* (2022) 219(6):1–23. doi: 10.1084/jem.20220011
- Milette S, Quail DF, Spicer JD. Neutrophil DNA webs untangled. *Cancer Cell* (2020) 38(2):164–6. doi: 10.1016/j.ccell.2020.07.002
- van Hezel ME, Boshuizen M, Peters AL, Straat M, Vlaar AP, Spoelstra-de Man AME, et al. Red blood cell transfusion results in adhesion of neutrophils in human endotoxemia and in critically ill patients with sepsis. *Transfusion* (2020) 60(2):294–302. doi: 10.1111/trf.15613
- Westerman TL, Sheats MK, Eifenbein JR. Sulfate import in salmonella typhimurium impacts bacterial aggregation and the respiratory burst in human neutrophils. *Infect Immun* (2021) 89(6):1–15. doi: 10.1128/IAI.00701-20
- Evani SJ, Karna SLR, Seshu J, Leung KP. Pirfenidone regulates LPS mediated activation of neutrophils. *Sci Rep* (2020) 10(1):19936. doi: 10.1038/s41598-020-76271-3
- de Almeida AD, Silva IS, Fernandes-Braga W, LimaFilho ACM, Florentino R, Barra A, et al. A role for mast cells and mast cell tryptase in driving neutrophil recruitment in LPS-induced lung inflammation via protease-activated receptor 2 in mice. *Inflammation Res* (2020) 69(10):1059–70. doi: 10.1007/s00011-020-01376-4
- McDonald PP, Bald A, Cassatella MA. Activation of the NF-kappaB pathway by inflammatory stimuli in human neutrophils. *Blood* (1997) 89(9):3421–33. doi: 10.1182/blood.V89.9.3421
- Nguyen-Jackson H, Panopoulos AD, Zhang H, Li HS, Watowich SS. STAT3 controls the neutrophil migratory response to CXCR2 ligands by direct activation of G-CSF-induced CXCR2 expression and via modulation of CXCR2 signal transduction. *Blood* (2010) 115(16):3354–63. doi: 10.1182/blood-2009-08-240317
- Malcolm KC, Arndt PG, Manos EJ, Jones DA, Worthen GS. Microarray analysis of lipopolysaccharide-treated human neutrophils. *Am J Physiol Lung Cell Mol Physiol* (2003) 284(4):L663–70. doi: 10.1152/ajplung.00094.2002
- Fessler MB, Malcolm KC, Duncan MW, Worthen GS. A genomic and proteomic analysis of activation of the human neutrophil by lipopolysaccharide and its mediation by p38 mitogen-activated protein kinase. *J Biol Chem* (2002) 277(35):31291–302. doi: 10.1074/jbc.M200755200
- Zhang X, Kluger Y, Nakayama Y, Poddar R, Whitney C, DeTora A, et al. Gene expression in mature neutrophils: early responses to inflammatory stimuli. *J Leukoc Biol* (2004) 75(2):358–72. doi: 10.1189/jlb.0903412

21. Coldren CD, Nick JA, Poch KR, Woolum MD, Fouty BW, O'Brien JM, et al. Functional and genomic changes induced by alveolar transmigration in human neutrophils. *Am J Physiol Lung Cell Mol Physiol* (2006) 291(6):L1267–76. doi: 10.1152/ajplung.00097.2006
22. Silva E, Arcaroli J, He Q, Svetkauskaite D, Coldren C, Nick JA, et al. HMGB1 and LPS induce distinct patterns of gene expression and activation in neutrophils from patients with sepsis-induced acute lung injury. *Intensive Care Med* (2007) 33(10):1829–39. doi: 10.1007/s00134-007-0748-2
23. Kotz KT, Xiao W, Miller-Graziano C, Qian WJ, Russom A, Warner EA, et al. Clinical microfluidics for neutrophil genomics and proteomics. *Nat Med* (2010) 16(9):1042–7. doi: 10.1038/nm.2205
24. de Kleijn S, Kox M, Sama IE, Pillay J, van Diepen A, Huijnen MA, et al. Transcriptome kinetics of circulating neutrophils during human experimental endotoxemia. *PLoS One* (2012) 7(6):e38255. doi: 10.1371/journal.pone.0038255
25. de Kleijn S, Langereis JD, Leentjens J, Kox M, Netea MG, Koenderman L, et al. IFN-gamma-stimulated neutrophils suppress lymphocyte proliferation through expression of PD-L1. *PLoS One* (2013) 8(8):e72249. doi: 10.1371/journal.pone.0072249
26. Khaenam P, Rinchai D, Altman MC, Chiche L, Buddhisa S, Kewcharoenwong C, et al. A transcriptomic reporter assay employing neutrophils to measure immunogenic activity of septic patients' plasma. *J Transl Med* (2014) 12:65. doi: 10.1186/1479-5876-12-65
27. Weigel D, Jackle H. The fork head domain: a novel DNA binding motif of eukaryotic transcription factors? *Cell* (1990) 63(3):455–6. doi: 10.1016/0092-8674(90)90439-L
28. Golson ML, Kaestner KH. Fox transcription factors: from development to disease. *Development* (2016) 143(24):4558–70. doi: 10.1242/dev.112672
29. Nagano S, Otsuka T, Nihiro H, Yamaoka K, Arinobu Y, Ogami E, et al. Molecular mechanisms of lipopolysaccharide-induced cyclooxygenase-2 expression in human neutrophils: involvement of the mitogen-activated protein kinase pathway and regulation by anti-inflammatory cytokines. *Int Immunol* (2002) 14(7):733–40. doi: 10.1093/intimm/14(7)733
30. Beyaert R, Cuenda A, Vanden Berghe W, Plaisance S, Lee JC, Haegeman G, et al. The p38/RK mitogen-activated protein kinase pathway regulates interleukin-6 synthesis response to tumor necrosis factor. *EMBO J* (1996) 15(8):1914–23. doi: 10.1002/j.1460-2075.1996.tb00542.x
31. Hunter T. Protein kinases and phosphatases: the yin and yang of protein phosphorylation and signaling. *Cell* (1995) 80(2):225–36. doi: 10.1016/0092-8674(95)90405-0
32. Zu Y-L, Qi J, Gilchrist A, Fernandez GA, Vazquez-Abad D, Kreutzer DL, et al. p38 mitogen-activated protein kinase activation is required for human neutrophil function triggered by TNF- α or FMLP stimulation. *J Immunol* (1998) 160(4):1982–9. doi: 10.4049/jimmunol.160.4.1982
33. Wang X, Qin W, Xu X, Xiong Y, Zhang Y, Zhang H, et al. Endotoxin-induced autocrine ATP signaling inhibits neutrophil chemotaxis through enhancing myosin light chain phosphorylation. *Proc Natl Acad Sci* (2017) 114(17):4483–8. doi: 10.1073/pnas.1616752114
34. Costa-Silva J, Domingues D, Lopes FM. RNA-Seq differential expression analysis: An extended review and a software tool. *PLoS One* (2017) 12(12):e0190152. doi: 10.1371/journal.pone.0190152
35. Kamp VM, Pillay J, Lammers JW, Pickkers P, Ulfman LH, Koenderman L. Human suppressive neutrophils CD16bright/CD62Ldim exhibit decreased adhesion. *J Leukoc Biol* (2012) 92(5):1011–20. doi: 10.1189/jlb.0611273
36. Batista F, Vaiman D, Dausset J, Fellous M, Veitia RA. Potential targets of FOXL2, a transcription factor involved in craniofacial and follicular development, identified by transcriptomics. *Proc Natl Acad Sci U S A* (2007) 104(9):3330–5. doi: 10.1073/pnas.0611326104
37. Scapini P, Laudanna C, Pinardi C, Allavena P, Mantovani A, Sozzani S, et al. Neutrophils produce biologically active macrophage inflammatory protein-3 α (MIP-3 α)/CCL20 and MIP-3 β /CCL19. *Eur J Immunol* (2001) 31(7):1981–8. doi: 10.1002/1521-4141(200107)31:7<1981::AID-IMMU1981>3.0.CO;2-X
38. Girbl T, Lenn T, Perez L, Rolas L, Barkaway A, Thiriot A, et al. Distinct compartmentalization of the chemokines CXCL1 and CXCL2 and the atypical receptor ACKR1 determine discrete stages of neutrophil diapedesis. *Immunity* (2018) 49(6):1062–76.e6. doi: 10.1016/j.immuni.2018.09.018
39. Massrieh W, Derjuga A, Doualla-Bell F, Ku CY, Sanborn BM, Blank V. Regulation of the MAFF transcription factor by proinflammatory cytokines in myometrial cells. *Biol Reprod* (2006) 74(4):699–705. doi: 10.1095/biolreprod.105.045450
40. Saliba J, Coutaud B, Solovieva V, Lu F, Blank V. Regulation of CXCL1 chemokine and CSF3 cytokine levels in myometrial cells by the MAFF transcription factor. *J Cell Mol Med* (2019) 23(4):2517–25. doi: 10.1111/jcmm.14136
41. Boespflug ND, Kumar S, McAlees JW, Phelan JD, Grimes HL, Hoebe K, et al. ATF3 is a novel regulator of mouse neutrophil migration. *Blood* (2014) 123(13):2084–93. doi: 10.1182/blood-2013-06-510909
42. Hai T, Wolfgang CD, Marsee DK, Allen AE, Sivaprasad U. ATF3 and stress responses. *Gene Expr* (1999) 7(4-6):321–35.
43. Liu CY, Chuang PI, Chou CL, Lin SM, Chen HC, Chou P, et al. Cytoprotective response of A1, a bcl-2 homologue expressed in mature human neutrophils and promyelocytic HL-60 cells, to oxidant stress-induced cell death. *J BioMed Sci* (2004) 11(2):214–27. doi: 10.1007/BF02256565
44. Arlt A, Schafer H. Role of the immediate early response 3 (IER3) gene in cellular stress response, inflammation and tumorigenesis. *Eur J Cell Biol* (2011) 90(6-7):545–52. doi: 10.1016/j.jecb.2010.10.002
45. Yang L, Froio RM, Sciuto TE, Dvorak AM, Alon R, Luscinskas FW. ICAM-1 regulates neutrophil adhesion and transcellular migration of TNF-alpha-activated vascular endothelium under flow. *Blood* (2005) 106(2):584–92. doi: 10.1182/blood-2004-12-4942
46. Elsakka NE, Webster NR, Galley HF. Polymorphism in the manganese superoxide dismutase gene. *Free Radic Res* (2007) 41(7):770–8. doi: 10.1080/10715760701338828
47. Prince LR, Prosseda SD, Higgins K, Carling J, Prestwich EC, Ogryzko NV, et al. NR4A orphan nuclear receptor family members, NR4A2 and NR4A3, regulate neutrophil number and survival. *Blood* (2017) 130(8):1014–25. doi: 10.1182/blood-2017-03-770164
48. Li S, Weidenfeld J, Morrissy EE. Transcriptional and DNA binding activity of the Foxp1/2/4 family is modulated by heterotypic and homotypic protein interactions. *Mol Cell Biol* (2004) 24(2):809–22. doi: 10.1128/MCB.24.2.809-822.2004
49. Carles A, Trigo-Gonzalez G, Cao Q, Cheng SG, Moks M, Bilenky M, et al. The pathogenomic FOXL2 C134W mutation alters DNA-binding specificity. *Cancer Res* (2020) 80(17):3480–91. doi: 10.1158/0008-5472.CAN-20-0104
50. Feng X, Ippolito GC, Tian L, Wiehagen K, Oh S, Sambandam A, et al. Foxp1 is an essential transcriptional regulator for the generation of quiescent naive T cells during thymocyte development. *Blood* (2010) 115(3):510–8. doi: 10.1182/blood-2009-07-232694
51. Feng X, Wang H, Takata H, Day TJ, Willen J, Hu H. Transcription factor Foxp1 exerts essential cell-intrinsic regulation of the quiescence of naive T cells. *Nat Immunol* (2011) 12(6):544–50. doi: 10.1038/ni.2034
52. Patzelt T, Keppler SJ, Gorka O, Thoene S, Wartewig T, Reth M, et al. Foxp1 controls mature b cell survival and the development of follicular and b-1 b cells. *Proc Natl Acad Sci U S A* (2018) 115(12):3120–5. doi: 10.1073/pnas.1711335115
53. Wiehagen KR, Corbo-Rodgers E, Li S, Staub ES, Hunter CA, Morrissy EE, et al. Foxp1 is dispensable for T cell development, but required for robust recall responses. *PLoS One* (2012) 7(8):e42273. doi: 10.1371/journal.pone.0042273
54. Shi C, Zhang X, Chen Z, Sulaiman K, Feinberg MW, Ballantyne CM, et al. Integrin engagement regulates monocyte differentiation through the forkhead transcription factor Foxp1. *J Clin Invest* (2004) 114(3):408–18. doi: 10.1172/JCI200421100
55. Gabut M, Samavarchi-Tehrani P, Wang X, Slobodeniuc V, O'Hanlon D, Sung HK, et al. An alternative splicing switch regulates embryonic stem cell pluripotency and reprogramming. *Cell* (2011) 147(1):132–46. doi: 10.1016/j.cell.2011.08.023
56. van Boxtel R, Gomez-Puerto C, Mokry M, Eijkelenboom A, van der Vos KE, Nieuwenhuis EE, et al. FOXP1 acts through a negative feedback loop to suppress FOXO-induced apoptosis. *Cell Death Differ* (2013) 20(9):1219–29. doi: 10.1038/cdd.2013.81
57. Greenberg DE, Sturdevant DE, Marshall-Batty KR, Chu J, Pettinato AM, Virtaneva K, et al. Simultaneous host-pathogen transcriptome analysis during granulobacter bethedensis infection of neutrophils from healthy subjects and patients with chronic granulomatous disease. *Infect Immun* (2015) 83(11):4277–92. doi: 10.1128/IAI.00778-15
58. Wright HJ, Chapple IL, Matthews JB, Cooper PR. Fusobacterium nucleatum regulation of neutrophil transcription. *J Periodontol Res* (2011) 46(1):1–12. doi: 10.1111/j.1600-0765.2010.01299.x
59. Richardson GM, Lannigan J, Macara IG. Does FACS perturb gene expression? *Cyto A* (2015) 87(2):166–75. doi: 10.1002/cyto.a.22608
60. Patel PN, Shah RY, Ferguson JF, Reilly MP. Human experimental endotoxemia in modeling the pathophysiology, genomics, and therapeutics of innate immunity in complex cardiometabolic diseases. *Arterioscler Thromb Vasc Biol* (2015) 35(3):525–34. doi: 10.1161/ATVBAHA.114.304455
61. Andreasen AS, Krabbe KS, Krogh-Madsen R, Taudorf S, Pedersen BK, Møller K. Human endotoxemia as a model of systemic inflammation. *Curr Med Chem* (2008) 15(17):1697–705. doi: 10.2174/092986708784872393
62. Tawfik DM, Lankelma JM, Vachot L, Cerrato E, Pachot A, Wiersinga WJ, et al. Comparison of host immune responses to LPS in human using an immune profiling panel, *in vivo* endotoxemia versus *ex vivo* stimulation. *Sci Rep* (2020) 10(1):9918. doi: 10.1038/s41598-020-66695-2
63. Wang B, Weidenfeld J, Lu MM, Maika S, Kuziel WA, Morrissy EE, et al. Foxp1 regulates cardiac outflow tract, endocardial cushion morphogenesis and myocyte proliferation and maturation. *Development* (2004) 131(18):4477–87. doi: 10.1242/dev.01287
64. Ewing B, Green P. Base-calling of automated sequencer traces using phred. II. error probabilities. *Genome Res* (1998) 8(3):186–94. doi: 10.1101/gr.8.3.186
65. Bolger AM, Lohse M, Usadel B. Trimmomatic: a flexible trimmer for illumina sequence data. *Bioinformatics* (2014) 30(15):2114–20. doi: 10.1093/bioinformatics/btu170
66. Kim D, Langmead B, Salzberg SL. HISAT: a fast spliced aligner with low memory requirements. *Nat Methods* (2015) 12(4):357–60. doi: 10.1038/nmeth.3317
67. Pertea M, Kim D, Pertea GM, Leek JT, Salzberg SL. Transcript-level expression analysis of RNA-seq experiments with HISAT, StringTie and ballgown. *Nat Protoc* (2016) 11(9):1650–67. doi: 10.1038/nprot.2016.095
68. Love MI, Huber W, Anders S. Moderated estimation of fold change and dispersion for RNA-seq data with DESeq2. *Genome Biol* (2014) 15(12):550. doi: 10.1186/s13059-014-0550-8
69. Thomas-Chollier M, Hufton A, Heinig M, O'Keefe S, Masri NE, Roeder HG, et al. Transcription factor binding predictions using TRAP for the analysis of ChIP-seq data and regulatory SNPs. *Nat Protoc* (2011) 6(12):1860–9. doi: 10.1038/nprot.2011.409
70. Brown PJ, Ashe SL, Leich E, Burek C, Barrans S, Fenton JA, et al. Potentially oncogenic b-cell activation-induced smaller isoforms of FOXP1 are highly expressed in the activated b cell-like subtype of DLBCL. *Blood* (2008) 111(5):2816–24. doi: 10.1182/blood-2007-09-115113
71. Wang B, Lin D, Li C, Tucker P. Multiple domains define the expression and regulatory properties of Foxp1 forkhead transcriptional repressors. *J Biol Chem* (2003) 278(27):24259–68. doi: 10.1074/jbc.M207174200
72. Louis Sam Titus ASC, Yusuff T, Cassar M, Thomas E, Kretschmar D, D'Mello SR. Reduced expression of Foxp1 as a contributing factor in huntington's disease. *J Neurosci* (2017) 37(27):6575–87. doi: 10.1523/JNEUROSCI.3612-16.2017
73. van Keimpema M, Grüneberg LJ, Schilder-Tol EJ, Oud ME, Beuling EA, Hensbergen PJ, et al. The small FOXP1 isoform predominantly expressed in activated b cell-like diffuse large b-cell lymphoma and full-length FOXP1 exert similar oncogenic and transcriptional activity in human b cells. *Haematologica* (2017) 102(3):573–83. doi: 10.3324/haematol.2016.156455